

1 **Spatiotemporally controlled genetic perturbation for**
2 **efficient large-scale studies of cell non-autonomous effects**

3

4

5 Andrea Chai^{1,2}, Ana M. Mateus^{1,2}, Fazal Oozeer¹, Rita Sousa-Nunes^{1,3}

6

7 ¹Centre for Developmental Neurobiology, Institute of Psychiatry, Psychology and
8 Neuroscience, King's College London, UK.

9 ²Equal contribution

10 ³To whom correspondence should be addressed: Rita.Sousa-Nunes@kcl.ac.uk

11

12

13 **Impact statement**

14 A novel genetic strategy for induction of reproducible neural tumors (or any
15 other deleterious phenotype) in a single *Drosophila* stock (applicable to other
16 organisms).

17

18

19 **Major subject areas, keywords, and research organism**

20 Cell non-autonomous effects, reproducible tumor, neural stem cell, *Drosophila*
21 *melanogaster*

22

23 **Abstract**

24 **Studies in genetic model organisms have revealed much about the**
25 **development and pathology of complex tissues. Most have focused on cell-**
26 **intrinsic gene functions and mechanisms. Much less is known about how**
27 **transformed, or otherwise functionally disrupted, cells interact with**
28 **healthy ones towards a favorable or pathological outcome. This is largely**
29 **due to technical limitations. We developed new genetic tools in *Drosophila***
30 ***melanogaster* that permit efficient multiplexed gain- and loss-of-function**
31 **genetic perturbations with separable spatial and temporal control.**
32 **Importantly, our novel tool-set is independent of the commonly used**
33 **GAL4/UAS system, freeing the latter for additional, non-autonomous,**
34 **genetic manipulations; and is built into a single strain, allowing one-**
35 **generation interrogation of non-autonomous effects. Altogether, our design**
36 **opens up efficient genome-wide screens on any deleterious phenotype.**
37 **Specifically, we developed tools to study extrinsic effects on neural tumor**
38 **growth but the strategy presented has endless applications within and**
39 **beyond neurobiology, and in other model organisms.**

40

41

42 **Introduction**

43 Despite numerous and versatile genetic mosaic strategies available for
44 genetically amenable model organism *Drosophila melanogaster*, none up to now
45 was suited for efficient large-scale screening for cell non-autonomous effects on
46 a developmentally deleterious genotype. Given the requirement for
47 combinations of genetic manipulations, non-autonomous effects are more
48 challenging to investigate yet well known to play crucial roles in development
49 and disease contexts such as cancer. The challenge applies to any tissue but is
50 particularly evident in the central nervous system (CNS) due to diversity of cell
51 types and uniqueness of each lineage with respect to gene expression, size,
52 projection patterns, as well as lethality frequently associated with their
53 disruption. A much needed, transformative, new tool would be: (i) a viable
54 parental stock in which (ii) chosen individual lineages could be (iii) triggered to
55 assume a deleterious genotype (iv) with temporal control (v) from which point
56 they would become permanently labeled by a reporter and (vi) with which a
57 single cross to existing stocks would produce progeny with genetically perturbed
58 cell types of interest other than the labeled lineages. To illustrate in our specific
59 case: no available genetic tool allowed large-scale screening for non-autonomous
60 effects on neural tumor growth as animals harbouring neural tumors cannot be
61 kept as a stable stock.

62 *Drosophila* has been a canvas for pioneering mosaic tools, at the heart of which
63 lie heterologous binary systems for transcriptional activation or recombination
64 (Griffin *et al.* 2014). Transcriptional activation systems include the yeast
65 transcription factor GAL4 and its binding site, named Upstream Activating

66 Sequence (UAS); the bacterial LexA/LexA Operator (LexAop); and the fungal
67 QF/QUAS system (Brand and Perrimon 1993; Yagi *et al.* 2010; Potter *et al.* 2010).
68 Recombination systems include the bacteriophage Cre recombinase and its loxP
69 target; the yeast Flippase/Flippase Recognition Target sites (FLP/FRT) and its
70 variant mFLP5/mFRT71; and other yeast recombinases (KD, R, B2, and B3) and
71 their cognate recognition sites (Golic and Linquist, 1989; Siegal and Hartl 1996;
72 Hadjieconomou *et al.* 2011; Nern *et al.*, 2011). The modularity of binary systems
73 grants them combinatorial flexibility, and ingenious Boolean logic gates between
74 recombination and transcriptional activation/silencing systems have expanded
75 their applications (eg., Struhl and Basler 1993; Lee and Luo 1999; Griffin *et al.*
76 2009; Yu *et al.* 2009; Yagi *et al.* 2010; Hadjieconomou *et al.* 2011; Hampel *et al.*
77 2011; von Philipsborn *et al.* 2011; Awasaki *et al.*, 2014). Binary systems have
78 been extensively employed to perform large-scale screens using publically
79 available UAS libraries to provide molecular understanding into numerous
80 conserved cell intrinsic processes (St Johnston 2002; Kawakami *et al.* 2016).
81 Genome-wide screens remain to be applied to extrinsic processes modifying an
82 adverse genotype.

83 We wished to determine the effects of microenvironment or systemic cues on
84 tumor progression. To this end we needed to generate reproducible neural
85 tumors in order to quantitatively assess growth. Tumor reproducibility requires
86 control over lineage, induction time and consistency of levels of downregulation
87 of tumor-suppressors and/or upregulation of oncogenes. We therefore aimed at
88 generating tumors in restricted lineage subsets with a fast inducing event in
89 parental (F0) animals, independently of GAL4/UAS so that we might employ this
90 binary system (for which most modules exist in *Drosophila*, including for near

91 genome-wide gain- and loss-of-function, readily available to the community) to
92 cause non-autonomous perturbations on F1 progeny. Due to possible fate
93 transformations and expression-level variations of regulatory sequences, we
94 wanted tumors to become irreversibly labeled under the control of a ubiquitous
95 and strong regulatory sequence from the time of induction. Various but not all of
96 these features can be achieved with suppressible/inducible LexA, Q and FLP
97 systems (Weigmann and Cohen 1999; Yagi *et al.* 2010; Riabinina *et al.* 2015).
98 Maintenance of an F0 stock with capacity for tumor induction requires
99 suppression of the deleterious genotype until desired. However, whilst the
100 *lexA^{GAD}* derivative (superscript indicating the GAL4 activation domain) can be
101 suppressed by GAL80, it is not compatible with continuous non-autonomous
102 gene inductions via GAL4 as these would also be affected. Also, alleviation of QF
103 suppression by quinic acid, or estrogen induction of FLP^{EBD} (superscript
104 indicating an estrogen-binding domain) requires ingestion and metabolization of
105 the effector molecule, resulting in relatively long induction kinetics and
106 variability, thus impairing reproducibility in the fast-developing fly tumor
107 models (Weigmann and Cohen 1999; Potter *et al.* 2010).

108 Our design presented achieves the desired features via the employment of two
109 very efficient transcriptional termination sequences (STOP cassettes) upstream
110 of an oncogenic sequence and reporter. Each STOP cassette is flanked by
111 recombinase target sequences selective for two distinct recombinases, one
112 constitutively expressed in selected lineages, conferring spatial specificity; the
113 other whose expression is induced by heat-shock (hs), conferring rapid temporal
114 resolution. We tested and refined the new genetic tools by recapitulating two
115 well-established *Drosophila* neural tumor models, one generated by

116 downregulation of the homeodomain transcription factor Prospero (Pros), which
117 can lead to tumorigenesis in all neural lineages (of which there are around 100
118 per central brain lobe); another by downregulation of the NHL-domain protein
119 Brain tumor (Brat), whose depletion leads to tumorigenesis specifically in so-
120 called type II lineages (of which there are eight per brain lobe ([Figure 1–figure](#)
121 [supplement 1](#)) (Sousa-Nunes *et al.* 2010). Starting from the units presented here
122 our design can be multiplexed beyond two to produce further spatial
123 intersections, or multiple temporal steps, along with any assemblies of gene
124 expression downstream (downregulation and/or upregulation, plus reporter
125 labeling). This strategy is therefore of broad interest, applicable to other tissues,
126 organisms and biological questions, opening-up large-scale screening for non-
127 autonomous effects.

128

129 **Results**

130 ***FOFO* tool design features**

131 Key to the design of this tumor-generating tool is that expression of deleterious
132 sequences by the ubiquitous strong *actin5C* promoter, was blocked by not one
133 (as commonly done), but two stringent STOP cassettes. Each STOP cassette was
134 flanked by the selective recombination sites FRT and mFRT71, specifically
135 recognized by FLP and mFLP5, respectively (Hadjieconomou *et al.* 2011). We
136 called this design “FOFO”, for Flp-Out-mFlp5-Out. The prediction was that
137 expression would be unblocked only in the presence of the two Flippases, with

138 spatiotemporal control achieved by lineage-restricted expression of FLP and hs-
139 induction of mFLP5 (Figure 1a).

140 We wanted our tumor-generating tool to induce expression not only of
141 oncogenes but to also allow downregulation of tumor suppressors, in addition to
142 a reporter gene (in this case enhanced green fluorescent protein, EGFP).
143 Multicistronic expression of oncogenic and reporter proteins can be easily
144 achieved by sandwiching T2A peptide (Gonzalez *et al.* 2011; Diao and White
145 2012) codons between coding sequences (cds). We therefore focused on
146 achieving a layout that reconciled strong reporter expression with gene
147 downregulation by short hairpin artificial microRNAs (miRs). Artificial miRs
148 consist of 21 bp sequences designed for RNA interference, embedded into a
149 sequence backbone of a naturally occurring miR; they are very effective in
150 downregulating gene expression (more so than long double-stranded RNAs; Ni *et*
151 *al.* 2011), can be transcribed by RNA polymerase II (Pol II) (Lee *et al.* 2014), and
152 can be concatenated for synergistic effect (Chen *et al.* 2007). We placed the EGFP
153 cds downstream of an intron as this increases transcript expression (Haley *et al.*
154 2010) and has the additional advantage of being able to host miRs without
155 disrupting transcript stability by their processing, unlike when miRs are placed
156 in the 3' untranslated region (3'UTR) (Bejarano *et al.* 2012).

157 Wishing to study strictly cell non-autonomous effects employing the GAL4/UAS
158 system, we included miRs targeting GAL4 as well as those targeting a tumor
159 suppressor (two miRs per target). Therefore, if the GAL4 expression domain
160 overlapped with the tumor domain, GAL4 would be silenced within the tumor.
161 miRs targeting the neural tumor suppressors *pros* or *brat* were used for tumor

162 induction and those targeting CD2 were used as control (Yu *et al.* 2009). To
163 minimize position effects and enhance expression, all constructs generated for
164 this study were flanked by gypsy insulators and integrated into the *Drosophila*
165 genome by PhiC3-mediated transgenesis, selecting sites reported to produce low
166 basal and high induced expression (Markstein *et al.* 2008).

167 The utility of this design lies in its combination with two distinct Flippases plus a
168 desired GAL4 transgene in a single organism (Figure 1b, F0 left). Once
169 assembled, this stock can then be crossed to any other carrying a UAS-transgene
170 (Figure 1b, F0 right). The spatially-restricted FLP will excise the first STOP
171 cassette with a domain reproducibility that depends on enhancer reliability and
172 strength as well as efficacy of the excision activity. In any case, neither reporter
173 nor deleterious sequences should be expressed due to the additional STOP
174 cassette. Consequently, until heat-shock, F0 and its F1 progeny should contain a
175 single mFLP5-Out cassette within the FLP-expressing domain. F1 should also
176 express the UAS-transgene in the GAL4 domain, and not express the miRs or
177 reporter (Figure 1b, F1 left). Following F1 heat-shock (Figure 1b, F1 middle), the
178 mFRT71-flanked STOP cassette should be excised (without spatial constraints,
179 its efficacy depending on heat-shock duration); following which the miRs and
180 reporter can be expressed but only within the FLP-expressing domain (Figure
181 1b, F1 right). If the GAL4 domain overlaps with the FLP spatial domain (as
182 schematized in Fig. 1b), strictly non-autonomous effects can still be studied since
183 GAL4 expression will be wiped-out therein by the GAL4^{miRs} (Figure 1b, F1 right).
184 A more naturalistic schematic illustrating brain tumours and GAL4 driven in all
185 glia is depicted in Figure 1c.

186

187 **Efficacy of STOP cassettes**

188 Central to the success of this strategy is the efficacy of the STOP cassettes. For
189 each we used tandem transcriptional terminators, as others before us. Whereas
190 some degree of STOP leakiness can be afforded to simply label cells or to
191 generate a deleterious genetic perturbation by means of a cross, it is absolutely
192 incompatible with our aim of harbouring a “locked” deleterious perturbation
193 within a stable stock. We tested a few transcriptional terminators until we
194 obtained the tightly controlled expression necessary.

195 Removal of the *lamin* cds from the STOP cassette used in Flybow
196 (Hadjieconomou *et al.* 2011) resulted in failure to terminate transcription
197 despite concatenated *hsp70Aa* and *hsp27* terminators, seen by EGFP expression
198 in the absence of Flippase (data not shown). In contrast, concatenation of
199 *hsp70Bb* and *SV40* terminators, successfully precluded unintended EGFP
200 expression. We therefore created a version of FOF0 (FOFO1.0) with the two
201 STOPs identical to the latter (Figure 2a). FOF01.0 was tested with publicly
202 available stocks of FLP and mFLP5 both under the control of the strong hs
203 promoter. Encouragingly, in the presence of both hs-FLP and hs-mFLP5 and only
204 after hs, extensive patches of EGFP were observed in all transgenics (*FOFO1.0-*
205 *CD2^{miRs}-GAL4^{miRs}*, *FOFO1.0-pros^{miRs}-GAL4^{miRs}* and *FOFO1.0-brat^{miRs}-GAL4^{miRs}*)
206 (Figure 2b). Furthermore, only in the presence of the oncogenic miRs were
207 ectopic neural stem cells (NSCs) observed (Figure 2b white-boxed insets: note
208 NSC density within EGFP patches in brains expressing oncogenic miRs versus
209 controls). However, ectopic NSCs were sometimes observed also outside the
210 EGFP domain in *FOFO1.0* carrying *pros^{miRs}* or *brat^{miRs}* (Figure 2b yellow-boxed

211 inset). Because this was never seen in the absence of hs it was a Flippase-
212 dependent process, likely due to inefficient termination of Pol II following
213 excision of only one of the STOP cassettes. We concluded that our design,
214 containing phenotype-inducing miRs ~200 bp downstream of STOP cassettes,
215 was a sensitive reporter of Pol II readthrough (Proudfoot 2016) and that this
216 STOP cassette was unsuitable for our purpose.

217 We next generated a FOF02.0 version containing two longer and potentially
218 stronger, STOP cassettes: the Flybow one including *lamin* cds and a
219 concatenation of four *SV40* terminators (Jackson *et al.* 2001; Hadjieconomou *et*
220 *al.* 2011). As with FOF01.0, in the presence of both hs-FLP and hs-mFLP5 and
221 only after hs, extensive patches of EGFP were observed in all FOF02.0
222 transgenics; and only in the presence of oncogenic miRs were ectopic NSCs
223 observed (Figure 2c white-boxed insets). This was the case for hs of 20 min and
224 1 h. When we performed a double hs of 1.5 h each 24 h apart on *FOFO2.0-*
225 *pros^{miRs}-GAL4^{miRs}* we occasionally saw tumors in the presence of only hs-mFLP5
226 (one central brain lineage in 8 out of 12 brains, which amounts to a frequency of
227 ~0.3 % as previously reported for cross-reactivity of hs-mFLP5 with FRT sites;
228 Hadjieconomou *et al.* 2011). To ascertain that there was no leaky *miR*
229 transcription in the absence of detectable EGFP, we counted the number of NSCs
230 per larval central brain lobe and saw no differences between wild-type (WT) and
231 *pros^{miRs}* and *brat^{miRs}* central brains, in the absence of hs or the presence of a
232 single Flippase (or, in the few cases where hs-mFLP5 cross-reacted with FRT
233 sites, outside the EGFP domain) (Figure 2-figure supplement 1). Crucially, with
234 FOF02.0 supernumerary NSCs were never observed outside the EGFP domain
235 (Figure 2c). In summary, the FOF02.0 design confirmed low-frequency cross-

236 reactivity between mFLP5 and FRT sites but largely blocked miR transcription in
237 the absence of either Flippase and successfully unblocked it in the presence of
238 both, with perfect correspondence to EGFP reporter expression.

239

240 **Functionality of *GAL4^{miRs}***

241 To test efficacy of *GAL4^{miRs}*, we crossed *hs-FLP; hs-mFLP5, FOF02.0-pros^{miRs}-*
242 *GAL4^{miRs}* flies to those where all neural lineages are labeled in GAL4/UAS-
243 dependent manner (GAL4 expressed in the domain of the Achaete-scute family
244 transcription factor Asense (Zhu *et al.* 2006; Bowman *et al.* 2008) in the genotype
245 *ase-GAL4, UAS-NLS::RFP*). The prediction was that wherever EGFP-labelled clones
246 would be induced (by heat-shock) the RFP signal would be wiped out due to co-
247 expression of *GAL4^{miRs}*. Indeed, following heat-shock, RFP-negative patches were
248 observed in perfect overlap with EGFP-labeled clones, as expected from efficient
249 GAL4 knock-down ([Figure 3](#)).

250 This experiment also illustrates successful combination of FLP/FOFO tools with
251 GAL4/UAS as intended for independent genetic manipulations and genome-wide
252 screens.

253

254 **New *enhancer-FLP(D)* transgenics**

255 The next step was to employ FOF02.0 to generate spatiotemporal controlled
256 tumors in the larval CNS. Because of the report that mFLP5 can act on FRT
257 sequences at low frequency but not the converse (Hadjieconomou *et al.* 2011),
258 we used FLP for constitutive spatial control (lineage-specific *enhancer-FLP*) and

259 mFLP5 for transiently-induced temporal control (*hs-mFLP5*). Few lineage-
260 specific FLP lines are currently available so we set out to generate some suited
261 for our purpose. For type II lineages, we used the *R19H09* and *stg¹⁴* enhancers
262 previously described to be expressed therein (Bayraktar *et al.* 2010; Wang *et al.*
263 2014). We then browsed images reporting larval CNS expression of a large
264 collection of *Drosophila* GAL4 lines (Manning *et al.* 2012) and selected twenty-six
265 with restricted expression for further analysis. Induction of *pros* or *brat* tumors
266 requires that these neural tumor suppressors be downregulated in progenitors,
267 not in differentiated progeny. We thus screened selected GAL4 lines for the
268 ability to induce supernumerary NSCs (inferred by larger reporter gene domain)
269 when crossed to *pros^{RNAi}* – a functional screen for expression in neural
270 progenitors. Ones of interest were further tested for the ability to induce
271 supernumerary NSCs also when crossed to *brat^{RNAi}*. Downregulation of *pros*
272 should induce supernumerary NSCs in all central brain lineages (type I or II)
273 whereas downregulation of *brat* should induce supernumerary NSCs only in type
274 II. Furthermore, because we aimed to generate lines to induce an irreversible
275 intrachromosomal recombination event, it was relevant to check not only
276 expression at a particular timepoint but the “complete” expression pattern from
277 onset, permanently reported by a FLP-out event. Altogether, we chose 9
278 enhancers from which to generate FLP lines (Figure 4–Figure supplement 1).

279 The degree of reproducibility of FOF0-induced tumors depends on
280 reproducibility of the expression domain of FLP, the strength of this expression
281 and recombination efficiency. We employed a mutated form of FLP called
282 FLP(D), which at position 5 contains an aspartic acid instead of glycine residue
283 (Babineau *et al.* 1985) and is reported to be at least ten-fold more efficient than

284 the original (Nern et al. 2011). Two different promoters were compared: that of
285 *hsp70* and the *Drosophila* Synthetic Core Promoter (DSCP) employed in the
286 generation of the GAL4 lines tested (Pfeiffer et al. 2008; Han et al. 2011). In all
287 cases, expression controlled by the *hsp70* promoter was less widespread relative
288 to that controlled by the DSCP (Figure 4), which could be due either to less
289 background or sensitivity. Aiming for spatial restriction, we used the *hsp70*
290 promoter lines for subsequent experiments.

291

292 **FLP cross-reactivity with mFRT71 at very low frequency**

293 Newly generated *enhancer-FLP* lines containing the *hsp70* promoter were tested
294 by crossing to *FOFO2.0-prosmiRs-GAL4miRs*. The prediction was that no induction of
295 supernumerary NSCs or EGFP expression would occur in progeny, whether or
296 not heat-shocked, since *hs-mFLP5* was not provided. Most lines behaved as
297 expected but some *enhancer-FLPs* did very occasionally lead to induction of EGFP
298 clusters containing supernumerary NSCs in the absence of hs. This indicates that
299 FLP can cross-react with very low frequency with non-cognate mFRT71 sites
300 (overall frequency of ~0.04 % based on the number of such clones within the
301 ~100 neural lineages per central brain). This cross-reactivity was never detected
302 when crossing *hs-FLP* alone to *FOFO2.0* lines even following long double heat-
303 shocks (Figure 2–supplement Figure 1), suggesting that this phenomenon is
304 either due to the FLP(D) structural variation, its enhanced recombination
305 efficiency, and/or the fact that it is provided constitutively by the spatially-
306 restricted enhancers as opposed to transiently via a hs-mediated pulse. In any

307 case, the almost negligible cross-reactivity indicated that these *enhancer-FLP*
308 lines could be used for our purpose.

309

310 ***FOFO2.0*-induced tumor reproducibility**

311 Each of the *FOFO2.0* transgenics (*FOFO2.0-CD2^{miRs}-GAL4^{miRs}*, *FOFO2.0-pros^{miRs}-*
312 *GAL4^{miRs}* and *FOFO2.0-brat^{miRs}-GAL4^{miRs}*) was next recombined with *hs-mFLP5*.

313 We then crossed these recombinants to *enhancer-FLP(D)* lines before combining

314 them into a single stock. As expected, EGFP-labelled supernumerary NSCs were

315 consistently observed following hs. It was possible to combine all transgenes in a

316 single animal stock with the exception of *R12H06-FLP(D)* and *FOFO2.0-pros^{miRs}-*

317 *GAL4^{miRs}*, which was the only one with a reasonable degree of tumor induction in

318 the absence of heat-shock (Figure 5–Supplement figure 1). The heat-shock

319 regime that led to best tumor reproducibility was a double pulse of 1.5 h each,

320 with the first at the end of embryogenesis and a second during L1 (when brain

321 NSCs are still quiescent), thus providing two doses of mFLP5 ~24 h apart

322 without intervening NSC divisions. Following heat-shock, patches of EGFP-

323 labelled supernumerary NSCs were observed for all enhancer-FLP(D) lines, with

324 both *hs-mFLP5;FOFO2.0-CD2^{miRs}-GAL4^{miRs}* (controls) and *hs-mFLP5;FOFO2.0-*

325 *pros^{miRs}-GAL4^{miRs}* but only the latter presented tumors (Figure 5). Concerning

326 *brat* tumors, with *hs-mFLP5;FOFO2.0-brat^{miRs}-GAL4^{miRs}* following heat-shock,

327 patches of EGFP-labelled supernumerary NSCs were efficiently generated

328 with *stg¹⁴-FLP(D)* but rarely observed for *R19H09-FLP(D)* (Figure 6; Figure

329 6–supplement figure 1) suggesting that the latter enhancer is relatively weak.

330 Concerning reproducibility, examples of various specimen for a type I NSC

331 *enhancer-FLP* and a type II NSC *enhancer-FLP* are shown (Figure 6). In summary
332 we were able to generate spatiotemporally-controlled lineage-restricted labeled
333 CNS tumors in a single stock in the absence of the GAL4/UAS system.

334

335 **Discussion**

336 We engineered genetic tools with which to generate labeled lineage-restricted
337 CNS tumors (applicable to any other deleterious genetic perturbation) in a single
338 stock, and independently of GAL4/UAS. We demonstrate successful combination
339 of novel FLP/FOFO tools with GAL4/UAS and efficacious GAL4 knock-down
340 within domains of FLP/mFLP5 and GAL4 intersection. This validates our tool for
341 independent genetic manipulations in strictly non-overlapping domains, which is
342 transformative for the study of cell non-autonomous effects. Our design opens up
343 for the first time the ability to perform efficient genome-wide screening for non-
344 autonomous effects on deleterious genotypes.

345 We show that employment of 4 miRs is efficacious and permits simultaneous
346 downregulation of multiple genes in the labeled domain; furthermore, T2A
347 sequences can be added for simultaneous overexpression of coding sequences in
348 addition to that for a reporter. The system can be used also to refine spatial
349 domains, intersecting various enhancer-recombinases (in addition or not to hs
350 control).

351 The sensitivity of our design (with miR expression inducing a readily detectable
352 and quantifiable phenotype even in non-labelled cells) allowed us to define STOP
353 cassettes appropriate to curb even short Pol II readthrough. The discrete number

354 of progenitors from which tumors are initiated provided a convenient platform
355 to quantify Flippase cross-reaction and revealed low-level cross-reaction of
356 FLP(D) with mFRT71 sites, not described before. The degree of tumor
357 reproducibility reported differences in strength and/or robustness of the
358 lineage-restricted enhancers (eg., as seen by non-symmetric *brat* tumors with
359 *R19H09-FLP(D)* versus bilaterally symmetric ones with *stg¹⁴-FLP(D)*).

360 With this setup, any desired GAL4 line can now be added to the stock containing
361 the other elements (spatially restricted-FLP, hs-mFLP5, FOF0) and screens can
362 be performed with a number of convenient criteria. For example, the presence of
363 larval neural tumors induces developmental delay whose extent is proportional
364 to tumor size (our unpublished observation); and in some lineages leads to adult
365 sub-lethality (i.e., presence of adults bearing tumors in a sub-Mendelian
366 proportion). Therefore, the extent of developmental delay and of adult escapers
367 can be used as first-pass proxies for tumor size, for speedy screening of non cell-
368 autonomous modifiers of these parameters. Tumor volume can be subsequently
369 measured directly. Additionally, a FOF0 version containing a Luciferase reporter
370 can be generated in order to use Luciferase activity as an efficient method of
371 quantifying reporter-expressing cells (in our case tumor volume) in
372 homogenized tissue (Homem *et al.* 2014).

373 Custom-made FOF0 tools can be applied to any desired topic and cell types.
374 Within the CNS, other examples include investigating cell non-autonomous
375 modifications of axon misguidance, perturbed arbor growth or synapse
376 formation, roles of glia on neurodegeneration, etc. Furthermore, even without
377 gene perturbations, the FOF0 tool allows sparse labeling of specifically targeted

378 cells (sparseness achieved by short heat-shock and cell-type targeting provided
379 by *enhancer-FLP*), which is extremely useful for studying cellular morphology
380 and/or migration. Beyond the CNS, the resurgence of interest in metabolism and
381 physiology, for example, has had strong contribution from *Drosophila* research
382 (Rajan and Perrimon 2013). These are disciplines that involve interplay between
383 cell types and different organs and tools like the ones described here will
384 undoubtedly propel them forward.

385 The principles of the FOFO design can be applied to other model organisms
386 where distinct site-specific recombinases work, such as is the case for zebrafish
387 and mouse (Nern *et al.* 2011; Femi *et al.* 2016; Carney and Mosimann 2018;
388 Yoshimura *et al.* 2018) for refined spatial and/or temporal control of gene
389 expression. In zebrafish, heat-shock induced gene expression allows for faster
390 and/or focal induction of gene expression as compared to drug-induced
391 expression (Halloran *et al.* 2000). Direct translation of a FOFO tool with the aim
392 here described (large-scale screening for non-autonomous effects) is feasible in
393 zebrafish by employment of the GAL4/UAS or Q/QUAS systems (Subedi *et al.*
394 2014; Kawakami *et al.* 2016). In mouse, one way thermal shock can be focally-
395 induced (thus minimizing unwanted damage of most cells) is by Brownian
396 motion of iron oxide nanoparticles when subject to a magnetic field. Once
397 injected into specific tissues, these nanoparticles remain static and can be
398 visualized by magnetic resonance imaging (Pankhurst *et al.* 2003), which means
399 the site of injection, and therefore of heat-shock, can be located any time post-
400 injection. Translating the example of this study into mice, induction of
401 tumorigenesis focally in specific cell types by a combination of heat-shock and a
402 cell-type specific recombinase, in a way that allows identification of exactly

403 where the tumor was initiated, will be invaluable to study the earliest events in
404 mammalian tumorigenesis. This is largely a “black box” in *in vivo* mammalian
405 cancer studies, with assumed extrapolation from *in vitro* findings, since by the
406 time a tumor can be visualized it is usually already of a substantially advanced
407 stage. FOFO applications are thus myriad and versatile.

408

409 **Materials and Methods**

410 **Plasmid backbone.** A modified *pCaSpeR* plasmid containing an *actin5C*
411 promoter and a PhiC31-Integrase *attB* site was kindly provided by C. Alexandre
412 and further modified as described next. To enhance expression and avoid
413 positional effects, gypsy insulators were amplified from *pVALIUM20*²⁴ adding 5'
414 EcoRI and XhoI, and 3' BamHI and NheI restriction sites: the gypsy PCR product
415 digested with EcoRI and NheI was cloned into identical sites in the modified
416 *pCaSpeR*, making *act5C-gypsy1*; the *gypsy* PCR product digested with XhoI and
417 BamHI was cloned into identical sites in *act5C-gypsy1*, making *act5C-gypsy2*. To
418 minimise recombination, this plasmid as well as its FOFO derivatives were best
419 grown in XL10-Gold Ultracompetent Cells (Agilent Technologies, Cat. No.
420 200314) at 30 °C at 150 rpm.

421 **FOFO modules.** An initial FOFO insert containing *CD2^{miRs}-GAL4^{miRs}* and
422 restriction sites at key locations for modularity was generated by gene synthesis
423 (Integrated DNA Technologies) and cloned into XhoI-NotI sites in *act5C-gypsy2*.

424 **Short hairpin design and exchange.** All miR sequences were embedded in the
425 *Drosophila miR-1* stem-loop backbone (Haley *et al.* 2008), within the *ftz* intron

426 (Haley *et al.* 2010). Control miRs were those previously used to downregulate
427 CD2 (Yu *et al.* 2009); both *GAL4 miRs* and one each for *pros* and *brat* were
428 sequences selected by the Transgenic RNAi Project (TRiP; Ni *et al.* 2011); other
429 *pros* and *brat miRs* were selected by us (sequences below) from the output of the
430 Designer of siRNA (DSIR) software (Vert *et al.* 2006;
431 <http://biodev.extra.cea.fr/DSIR/DSIR.html>). In brief, target mRNA sequences
432 were fed into the software and output sequences BLASTed against the *Drosophila*
433 transcriptome; sequences with ≥ 16 -bp contiguous matches to other targets
434 were excluded. Hairpin sequences targeting *pros* or *brat* along with ones
435 targeting *GAL4*, flanked by *AscI* on the 5' end and *AvrII* on the 3' end, were
436 generated by gene synthesis (GenScript). The *AscI*-*AvrII* fragments were cloned
437 into identical sites in FOF01.0, making *FOF01.0-pros^{miRs}-GAL4^{miRs}* or *FOF01.0-*
438 *brat^{miRs}-GAL4^{miRs}*. The restriction sites (lowercase) and hairpin sequences (sense
439 and antisense indicated in **bold**) used in this study were:

440 *GAL4^{miRs}*:

441 cctagAACATCCCATAAAACATCCCATATTCAGCCGCTAGCAGT**CAGGATTATTTGT**
442 **ACAAGATATAGTTATATTCAAGCATATATCTTGTACAAATAATCCTGGCGAATTC**
443 AGGCGAGACATCGGAGTTGAAACTAAACTGAAATTTACTAGAAAACATCCCATAAA
444 ACATCCCATATTCAGCCGCTAGCAGT**TCGGAAGAGAGTAGTAACAAATAGTTATAT**
445 TCAAGCATATTT**GTTACTACTCTCTCCGAGCGAATTCAGGCGAGACATCGGAGTT**
446 GAAACTAAACTGAAATTT**CCTAGG**

447 *pros^{miRs}*:

448 ggcgcgccAACATCCCATAAAACATCCCATATTCAGCCGCTAGCAGT**CAGGATGTGGA**
449 **ACAAGAACAATAGTTATATTCAAGCATATTGTTCTTGTTCACATCCTGGCGAATT**

450 CAGGCGAGACATCGGAGTTGAAACTAAAAGTAAATTTACTAGAAAACATCCCATAA
451 AACATCCCATATTCAGCCGCTAGCAGTTAGCAGTAGTAGTAACAATAATAGTTATA
452 TTCAAGCATATTATTGTTACTACTACTGCTAGCGAATTCAGGCGAGACATCGGAGT
453 TGAAACTAAAAGTAAATTTCTAGG

454 *brat*^{miRs}:

455 ggcgcgccAACATCCCATAAAAACATCCCATATTCAGCCGCTAGCAGTCTGTGTCAAGGT
456 GTTCAACTATAGTTATATTCAAGCATATAGTTGAACACCTTGACACAGGCGAATTC
457 AGGCGAGACATCGGAGTTGAAACTAAAAGTAAATTTACTAGAAAACATCCCATAAAA
458 ACATCCCATATTCAGCCGCTAGCAGTGGCGTGGTGGTCAACGACAATAGTTATAT
459 TCAAGCATATTGTCGTTGACCACCACGCCGCGAATTCAGGCGAGACATCGGAGTT
460 GAAACTAAAAGTAAATTTCTAGG

461 **STOP cassettes.** FOF01.0 contained two identical STOP cassettes consisting of
462 *hsp70Bb* (Nern *et al.* 2011) and *SV40* terminators. FOF02.0 contained a first
463 STOP cassette consisting of the *lamin* cds plus *hsp70Aa* and *hsp27 polyA*
464 generated by PCR using FB2.0 (Hadjieconomou *et al.* 2011) as template with the
465 primers (Forward and Reverse always indicated in this order): gat cga tcc ccg ggt
466 acc gcg gcc gcA TAG GGA ATT GGG AAT TCG C and cga att ccc aat tcc cgt tta aAc
467 TCG AGG GTA CCA GAT CTG (uppercase indicating complementarity to
468 template); and a second STOP cassette consisting of four tandem *SV40 polyA*
469 sequences generated by PCR using the plasmid *Lox-Stop-Lox TOPO* (Addgene;
470 Jackson *et al.* 2001) as template with the primers: gat cga tcc ccg ggt acc gcg gcc
471 gcG AAG TTC CTA TAC TTT CTA G and ttt ggc ttt agt cga CTC TAG TTT AGG CGT
472 AAT CG. Products were inserted by Gibson Assembly (NEB) into *FOFO-EGFPnls*
473 backbones digested with NotI and PmeI to remove the existing STOP cassettes.

474 Primers were designed either manually or, for Gibson Assembly, with the New
475 England Biolabs builder tool (<http://nebuilder.neb.com/>).

476 **Reporter.** The reporter gene used was EGFP, fused in its N-terminal to a
477 membrane targeting sequence (CD8), obtained by PCR from FB2.0
478 (Hadjieconomou *et al.* 2011); or in its C-terminal to the SV40 NLS
479 GSPPKKKRKVEDV (GGA TCC CCC CCC AAG AAG AAG CGC AAG GTG GAG GAC GTC
480 TAG) engineered by Gibson Assembly (New England Biolabs) from a sequence
481 kindly provided by G. Struhl and including a Kozak consensus. The 3'UTR used
482 was *His2av3'UTR*-PolyA (Manning *et al.* 2012).

483 **Enhancer-FLPs.** For the *enhancer-FLP(D)* constructs, the plasmid *pDEST-*
484 *HemmarG* (Addgene; Han *et al.* 2011) was modified using Gibson Assembly (New
485 England Biolabs) as described next. *CD4-tdGFP cds* was removed with XhoI and
486 XbaI and replaced by a PCR fragment encoding FLP(D) obtained from *pJFRC150-*
487 *20XUAS-IVS-Flp1::PEST* (Addgene; Nern *et al.* 2011) with the primers: cct ttt cgt
488 tta gcc aag act cga gAA TCA AAA TGC CGC AGT TTG and act ggc tta gtt aat taa ttc
489 tag att aAA TAC GGC GAT TGA TGT AG. We call the resulting plasmid *pDEST-*
490 *Hemmar-FLP(D)*. This was transformed into One Shot® *ccdB Survival™ 2 T1R*
491 Competent Cells (Life Technologies, Cat. No. A10460). A modified version of
492 *pDEST-Hemmar-FLP(D)* containing the *DSCP* promoter (Pfeiffer *et al.* 2008) and
493 the *ftz* intron (Haley *et al.* 2010) was generated using Gibson Assembly (New
494 England Biolabs) using *pBPGUw* as a template. *pDEST-HemmarG* was digested
495 with Bbvcl and XbaI, removing part of the *ccdB cds* as well as the *hsp70*
496 promoter, the *zeste* intron and *CD4-tdGFP cds*. PCR fragments containing the
497 sequences for completing the *ccdB cds* as well as for the *DSCP* promoter, *ftz*

498 intron and *FLP(D)* *cds* were obtained using the primers: gga aaa tca gga agg gat
499 ggc tga ggT CGC CCG GTT TAT TGA AAT G and cgg cca att cAG CTG AAC GAG AAA
500 CGT AAA ATG (*attR1 + ccdB cds*), tcg ttc agc tGA ATT GGC CGC GTT TAA AC and
501 gat tct cga gCC TGC AGG TCT TTG CAA TC (*DSCP* and *ftz* intron), gac ctg cag gCT
502 CGA GAA TCA AAA TGC C and act ggc tta gtt aat taa ttc tag atc tag att aAA TAC
503 GGC GAT TGA TGT AG (*FLP(D)* *cds*) and assembled into the Bbvcl-XbaI *pDEST-*
504 *HemmarG* fragment. We call the resulting plasmid *pDEST-Hemmar-DSCP-ftz-*
505 *FLP(D)*.

506 Enhancer fragments were generated by PCR from gDNA and cloned into
507 *pENTR/D-TOPO* (Life Technologies, Cat. No. K2400-20). Primer sequences
508 contained CACC at the 5' end of the forward primer for Gateway cloning. LR
509 reaction products between *pENTR/D-TOPO* containing enhancer fragments and
510 *pDEST-Hemmar-FLP(D)* or *pDEST-Hemmar-DSCP-ftz-FLP(D)* were used to
511 generate transgenic flies.

512 ***Drosophila* stocks and transgenesis.** *hs-FLP*, *UAS-CD8::GFP*, *UAS-brat^{SH}*, *UAS-*
513 *pros^{SH}/CyO* and Janelia Farm GAL4 lines were obtained from the Bloomington
514 Stock Centre; *act>STOP>GAL4,UAS-GFP* was a gift from W. Chia; *UAS-*
515 *FLP,tub>STOP>Gal4,UAS-CD8::GFP* was a gift from M. Landgraf; *ase-GAL4*
516 recombined with *UAS-myr::RFP* was a gift from A. Bailey. *Bc/CyO*; *hs-mFLP5/TM2*
517 was a gift from I. Salecker.

518 PhiC31 Integrase-mediated transgenesis was performed by BestGene Inc. into
519 *attP40 (FOFO)*, *attP18 (enhancer-FLP)*, *attP16 (hs-FLP or hs-mFLP5)* strains
520 mutant for the gene *white*, which results in white eyes; since all transgenes

521 included the *white* gene, insertions were selected by eye color in the F1
522 generation. For *FOFO* transgenesis, animals were injected and reared at 18 °C.

523 **Heat-shocks.** Larvae were heat-shocked by tube emersion into a 37 °C water-
524 bath. Duration as indicated in text and/or figures.

525 **Immunohistochemistry and imaging.** For immunohistochemistry, CNSs were
526 fixed for 15 min in 3.7% formaldehyde in PBS. Mouse anti-Miranda (mAb81
527 1/50; gift from F. Matsuzaki) was used to label NSCs. Secondary antibodies were
528 conjugated to either Alexa-Fluor-488 or Alexa-Fluor-555 (Molecular Probes) and
529 used at 1/500. DNA stain was TO-PRO3 iodide (Molecular Probes). Tissues were
530 mounted in Vectashield (Vector Laboratories) and images obtained using a Zeiss
531 LSM510 confocal microscope. Images were acquired using the same confocal
532 (laser power, gain and pinhole) conditions. Maximum intensity z-stack
533 projections were generated and brightness/contrast of whole images adjusted
534 with FIJI software.

535 **Quantifications and statistics.** No randomization nor blinding was used except
536 for data shown in Supplementary Figure 2, where NSC counts were performed
537 blind for genotype. Here, each data point corresponds to a different individual of
538 the designated genotype or condition. Sample size calculation is unwarranted
539 due to the small standard deviation of the number of NSCs per central brain lobe
540 in WT and the large effect that tumour induction has on this (many standard
541 deviations above the mean). Each experiment was performed twice (biological
542 replicates). Biological replicates refer to biologically distinct samples
543 (independent crosses) grown in the same conditions and undergone the
544 experimental procedure; sample number is indicated in each appropriate figure

545 legend. Data was checked for normalcy via the Liliefors test; significance of
546 difference between each genotype and WT was tested by Ordinary One Way
547 ANOVA, multiple comparisons. No data was excluded. Statistical tests and graphs
548 were generated using Prism software.

549

550 **Author contributions**

551 A.M. and F.O. generated constructs. A.M. performed preliminary experiments
552 with FOF01.0 and acquired some of the data in Supplementary Figure 3. A.C.
553 acquired all other data shown. A.C., A.M. and R.S.-N. analysed and interpreted
554 data. R.S.-N. was responsible for the concept, design and supervision of the
555 project, and wrote the manuscript, which all authors revised.

556

557 **Acknowledgments**

558 We thank C. Alexandre, A. Bailey, W. Chia, B. Haley, M. Landgraf, I. Salecker and G.
559 Struhl for reagents or advice; and T. Carter, K. Chester, J. Clarke, M. Fanto, T.E.
560 Rusten, and D. Schmucker for helpful comments on the manuscript. We are also
561 grateful to N. Carvajal, M.J. Cruz and A. Miedzik and for technical assistance with
562 some experiments.

563

564 **Funding**

565 This work was supported by a Cancer Research UK Career Development
566 Fellowship to R.S.-N., which then supported also A.C. and A.M.. The funding
567 source was not involved in study design, data collection and interpretation, nor
568 the decision to submit the work for publication.

569

570 **Competing Interests**

571 The authors declare no financial or non-financial competing interests.

572

573 **References**

574 Awasaki, A., Kao, C.F., Lee, Y.J., Yang, C.P., Huang, Y., Pfeiffer, B.D., Luan, H., Jing,
575 X., Huang, Y.F., He, Y., Schroeder, M.D., Kuzin, A., Brody, T., Zugates,
576 C.T., Odenwald, W.F., Lee, T. Making *Drosophila* lineage-restricted drivers
577 via patterned recombination in neuroblasts. *Nat. Neurosci.* **17**, 631-637
578 (2014).

579 Babineau, D., Vetter, D., Andrews, B.J., Gronostajski, R.M., Proteau, G.A., Beatty,
580 L.G., Sadowski, P.D. The FLP protein of the 2-micron plasmid of yeast.
581 Purification of the protein from *Escherichia coli* cells expressing the cloned
582 FLP gene. *J. Biol. Chem.* **260**, 12313-12319 (1985).

583 Bayraktar, O.A., Boone, J.Q., Drummond, M.L., Doe, C.Q. *Drosophila* type II
584 neuroblast lineages keep Prospero levels low to generate large clones that
585 contribute to the adult brain central complex. *Neural Dev.* **5**, 26 (2010).

- 586 Bejarano, F., Bortolamiol-Becet, D., Dai, Q., Sun, K., Saj, A., Chou, Y.T., Raleigh,
587 D.R., Kim, K., Ni, J.Q., Duan, H., Yang, J.S., Fulga, T.A., Van Vactor,
588 D., Perrimon, N., Lai, E.C. A genome-wide transgenic resource for
589 conditional expression of *Drosophila* microRNAs. *Development* **139**, 2821-
590 2831 (2012).
- 591 Bowman, S.K., Rolland, V., Betschinger, J., Kinsey, K.A., Emery, G., Knoblich, J.A.
592 The Tumor Suppressors Brat and Numb Regulate Transit-Amplifying
593 Neuroblast Lineages in *Drosophila*. *Dev. Cell* **14**, 535-546 (2008).
- 594 Brand, A.H., Perrimon, N. Targeted gene expression as a means of altering cell
595 fates and generating dominant phenotypes. *Development* **118**, 401-415
596 (1993).
- 597 Carney, T.J., Mosimann, C. Switch and Trace: Recombinase Genetics in Zebrafish.
598 *Trends Genetics* **34**, 362-278(2018).
- 599 Chen, C.H., Huang, H., Ward, C.M., Su, J.T., Schaeffer, L.V., Guo, M., Hay, B.A. A
600 Synthetic Maternal-Effect Selfish Genetic Element Drives Population
601 Replacement in *Drosophila*. *Science* **316**, 597-600 (2007).
- 602 Diao, F., White, B.H. Novel Approach for Directing Transgene Expression in
603 *Drosophila*: T2A-Gal4 In-Frame Fusion. *Genetics* **190**, 1139-1144 (2012).
- 604 Femi J. Olorunniji, F.J., Rosser, S.J., Stark, W.M. Site-specific recombinases:
605 molecular machines for the Genetic Revolution. *Biochem. J.* **473**, 673-684
606 (2016).
- 607 Golic, K.G., Lindquist, S. The FLP recombinase of yeast catalyzes site-specific
608 recombination in the *Drosophila* genome. *Cell* **59**, 499-509 (1989).

- 609 Gonzalez, M., Martín-Ruiz, I., Jiménez, S., Pirone, L., Barrio, R., Sutherland, J.D.
610 Generation of stable *Drosophila* cell lines using multicistronic vectors. *Sci*
611 *Rep* **1**, 75 (2011).
- 612 Griffin, R., Binari, R., Perrimon, N. Genetic odyssey to generate marked clones in
613 *Drosophila* mosaics. *Proc. Natl. Acad. Sci. USA* **111**, 4756-4763 (2014).
- 614 Griffin, R., Sustar, A., Bonvin, M., Binari, R., del Valle Rodriguez, A., Hohl,
615 A.M., Bateman, J.R., Villalta, C., Heffern, E., Grunwald, D., Bakal, C., Desplan,
616 C., Schubiger, G., Wu, C.T., Perrimon, N. The twin spot generator for
617 differential *Drosophila* lineage analysis. *Nat. Methods* **6**, 600-602 (2009).
- 618 Hadjieconomou, D., Rotkopf, S., Alexandre, C., Bell, D.M., Dickson, B.J., Salecker, I.
619 Flybow: genetic multicolor cell labeling for neural circuit analysis in
620 *Drosophila melanogaster*. *Nat. Methods* **8**, 260-266 (2011).
- 621 Haley, B., Foys, B., Levine, M. Vectors and parameters that enhance the efficacy of
622 RNAi-mediated gene disruption in transgenic *Drosophila*. *Proc. Natl. Acad.*
623 *Sci. USA* **107**, 11435-11440 (2010).
- 624 Haley, B., Hendrix, D., Trang, V., Levine, M. (2008). A simplified miRNA-based
625 gene silencing method for *Drosophila melanogaster*. *Dev. Biol.* **321**, 482-490
626 (2008).
- 627 Halloran, M.C., Sato-Maeda, M., Warren Jr, J.T., Su, F., Lele, Z., Krone, P.H., Kuwada,
628 J.Y., Shoji, W. Laser-induced gene expression in specific cells of transgenic
629 zebrafish. *Development* **127**, 1953-1960 (2000).
- 630 Hampel, S., Chung, P., McKellar, C.E., Hall, D., Looger, L.L., Simpson, J.H. *Drosophila*
631 Brainbow: a recombinase-based fluorescence labeling technique to
632 subdivide neural expression patterns. *Nat. Methods* **8**, 253-259 (2011).

- 633 Han, C., Jan, L.Y., Jan, Y.N. Enhancer-driven membrane markers for analysis of
634 nonautonomous mechanisms reveal neuron-glia interactions in *Drosophila*.
635 *Proc. Natl. Acad. Sci. USA* **108**, 9673-9678 (2011).
- 636 Homem, C.C.F., Steinmann, V., Burkard, T.R., Jais, A., Esterbauer, H., Knoblich, J.A..
637 Ecdysone and Mediator Change Energy Metabolism to Terminate
638 Proliferation in *Drosophila* Neural Stem Cells. *Cell* **158**, 874-888 (2014).
- 639 Jackson, E.L., Willis, N., Mercer, K., Bronson, R.T., Crowley, D., Montoya, R., Jacks,
640 T., Tuveson, D.A. Analysis of lung tumor initiation and progression using
641 conditional expression of oncogenic K-ras. *Genes Dev.* **15**, 3243-3248
642 (2001).
- 643 Kawakami, K., Asakawa, K., Hibi, M., Itoh, M., Muto, A., Wada, H. Gal4 Driver
644 Transgenic Zebrafish: Powerful Tools to Study Developmental Biology,
645 Organogenesis, and Neuroscience. *Adv. Genet.* **95**, 65-87 (2016).
- 646 Lee, T., Luo, L. Mosaic analysis with a repressible cell marker for studies of gene
647 function in neuronal morphogenesis, *Neuron* **22**, 451-461 (1999).
- 648 Lee, Y., Kim, M., Han, J., Yeom, K.H., Lee, S., Baek, S.H., Kim, V.N. MicroRNA genes
649 are transcribed by RNA polymerase II. *EMBO J.* **23**, 4051-4060 (2004).
- 650 Manning, L., Heckscher, E.S., Purice, M.D., Roberts, J., Bennett, A.L., Kroll, J.R.,
651 Pollard, J.L., Strader, M.E., Lupton, J.R., Dyukareva, A.V., Doan, P.N., Bauer,
652 D.M., Wilbur, A.N., Tanner, S., Kelly, J.J., Lai, S.L., Tran, K.D., Kohwi, M.,
653 Lavery, T.R., Pearson, J.C., Crews, S.T., Rubin, G.M., Doe, C.Q. A resource for
654 manipulating gene expression and analyzing cis-regulatory modules in the
655 *Drosophila* CNS. *Cell Rep.* **2**, 1002-1013 (2012).

- 656 Markstein, M., Pitsouli, C., Villalta, C., Celniker, S.E., Perrimon, N. Exploiting
657 position effects and the gypsy retrovirus insulator to engineer precisely
658 expressed transgenes. *Nat. Genet.* **40**, 476-483 (2008).
- 659 McGuire, S.E., Le, P.T., Osborn, A.J., Matsumoto, K., Davis, R.L. Spatiotemporal
660 rescue of memory dysfunction in *Drosophila*. *Science* **302**, 1765-1768
661 (2003).
- 662 Nern, A., Pfeiffer, B.D., Svoboda, K., Rubin, G.M. Multiple new site-specific
663 recombinases for use in manipulating animal genomes. *Proc. Natl. Acad. Sci.*
664 *USA* **108**, 14198-14203 (2011).
- 665 Ni, J.Q., Zhou, R., Czech, B., Liu, L.P., Holderbaum, L., Yang-Zhou, D., Shim,
666 H.S., Tao, R., Handler, D., Karpowicz, P., Binari, R., Booker, M., Brennecke, J.,
667 Perkins, L.A., Hannon, G.J., Perrimon, N. A genome-scale shRNA resource for
668 transgenic RNAi in *Drosophila*. *Nat. Methods* **8**, 405-407 (2011).
- 669 Pankhurst, Q.A., Connolly, J., Jones, S.K., Dobson J. Applications of magnetic
670 nanoparticles in biomedicine. *J. Phys. D: Appl. Phys.* **36**, R167–R181 (2003).
- 671 Pfeiffer, B.D., Jenett, A., Hammonds, A.S., Ngo, T.T., Misra, S., Murphy, C., Scully, A.,
672 Carlson, J.W., Wan, K.H., Lavery, T.R., Mungall, C., Svirskas, R., Kadonaga,
673 J.T., Doe, C.Q., Eisen, M.B., Celniker, S.E., Rubin, G.M. Tools for neuroanatomy
674 and neurogenetics in *Drosophila*. *Proc. Natl. Acad. Sci. USA* **105**, 9715–9720
675 (2008).
- 676 Potter, C.J., Tasic, B., Russler, E.V., Liang, L., Luo, L. The Q System: A Repressible
677 Binary System for Transgene Expression, Lineage Tracing, and Mosaic
678 Analysis. *Cell* **141**, 536-548 (2010).
- 679 Proudfoot, N.J. Transcriptional termination in mammals: Stopping the RNA
680 polymerase II juggernaut. *Science* **352**, aad9926-1-aad9926-9 (2016).

- 681 Rajan, A., Perrimon, N. Of flies and men: insights on organismal metabolism from
682 fruit flies. *BMC Biol.* **11**, 38 (2013).
- 683 Riabinina, O., Luginbuhl, D., Marr, E., Liu, S., Wu, M.N., Luo, L., Potter, C.J.
684 Improved and expanded Q-system reagents for genetic manipulations. *Nat.*
685 *Methods* **12**, 219-222 (2015).
- 686 Siegal, M.L., Hartl, D.L. Transgene Coplacement and high efficiency site-specific
687 recombination with the Cre/loxP system in *Drosophila*. *Genetics* **144**, 715-
688 726 (1996).
- 689 Sousa-Nunes, R., Cheng, L.Y., Gould, A.P. Regulating neural proliferation in the
690 *Drosophila* CNS. *Curr. Opin. Neurobiol.* **20**, 50-57 (2010).
- 691 St Johnston, D. The art and design of genetic screens: *Drosophila melanogaster*.
692 *Nat. Rev. Genet.* **3**, 176-188 (2002).
- 693 Struhl, G., Basler, K. Organizing activity of wingless protein in *Drosophila*. *Cell* **72**,
694 527-540 (1993).
- 695 Subedi, A., Macurak, M., Gee, S.T., Monge, E., Goll, M.G., Potter, C.J., Parsons, M.J.,
696 Halpern, M.E. Adoption of the Q transcriptional regulatory system for
697 zebrafish transgenesis. *Methods* **66**, 433-440 (2014).
- 698 Vert, J.P., Foveau, N., Lajaunie, C., Vandenbrouck, Y. An accurate and interpretable
699 model for siRNA efficacy prediction. *BMC Bioinformatics* **7**, 520 (2006).
- 700 von Philipsborn, A.C., Liu, T., Yu, J.Y., Masser, C., Bidaye, S.S., Dickson, B.J.
701 Neuronal Control of *Drosophila* Courtship Song. *Neuron* **69**, 509-522
702 (2011).
- 703 Wang, Y.C., Yang, J.S., Johnston, R., Ren, Q., Lee, Y.J., Luan, H., Brody, T., Odenwald,
704 W.F., Lee, T. *Drosophila* intermediate neural progenitors produce lineage-

705 dependent related series of diverse neurons. *Development* **141**, 253-258
706 (2014).

707 Weigmann, K., Cohen, S.M. Lineage-tracing cells born in different domains along
708 the PD axis of the developing *Drosophila* leg. *Development* **126**, 3823-3830
709 (1999).

710 Yagi, R., Mayer, F., Basler, K. Refined LexA transactivators and their use in
711 combination with the *Drosophila* Gal4 system. *Proc. Natl. Acad. Sci. USA*
712 **107**, 16166-16171 (2010).

713 Yoshimura, Y., Ida-Tanaka, M., Hiramaki, T., Goto, M., Kamisako, T., Eto, T., Yagoto,
714 M., Kawai, K., Takahashi, T., Nakayama, M., Ito, M. Novel reporter and
715 deleter mouse strains generated using VCre/VloxP and SCre/SloxP
716 systems, and their system specificity in mice. *Transgenic Res.* **27**, 193-201
717 (2018).

718 Yu, H.-H., Chen, C.-H., Shi, L., Huang, Y., Lee, T. Twin-spot MARCM to reveal the
719 developmental origin and identity of neurons. *Nat. Neurosci.* **12**, 947-953
720 (2009).

721 Zhu, S., Lin, S., Kao, C.F., Awasaki, T., Chiang, A.S., Lee, T. Gradients of the
722 *Drosophila* Chinmo BTB-Zinc Finger Protein Govern Neuronal Temporal
723 Identity. *Cell* **127**, 409-422 (2006).

724

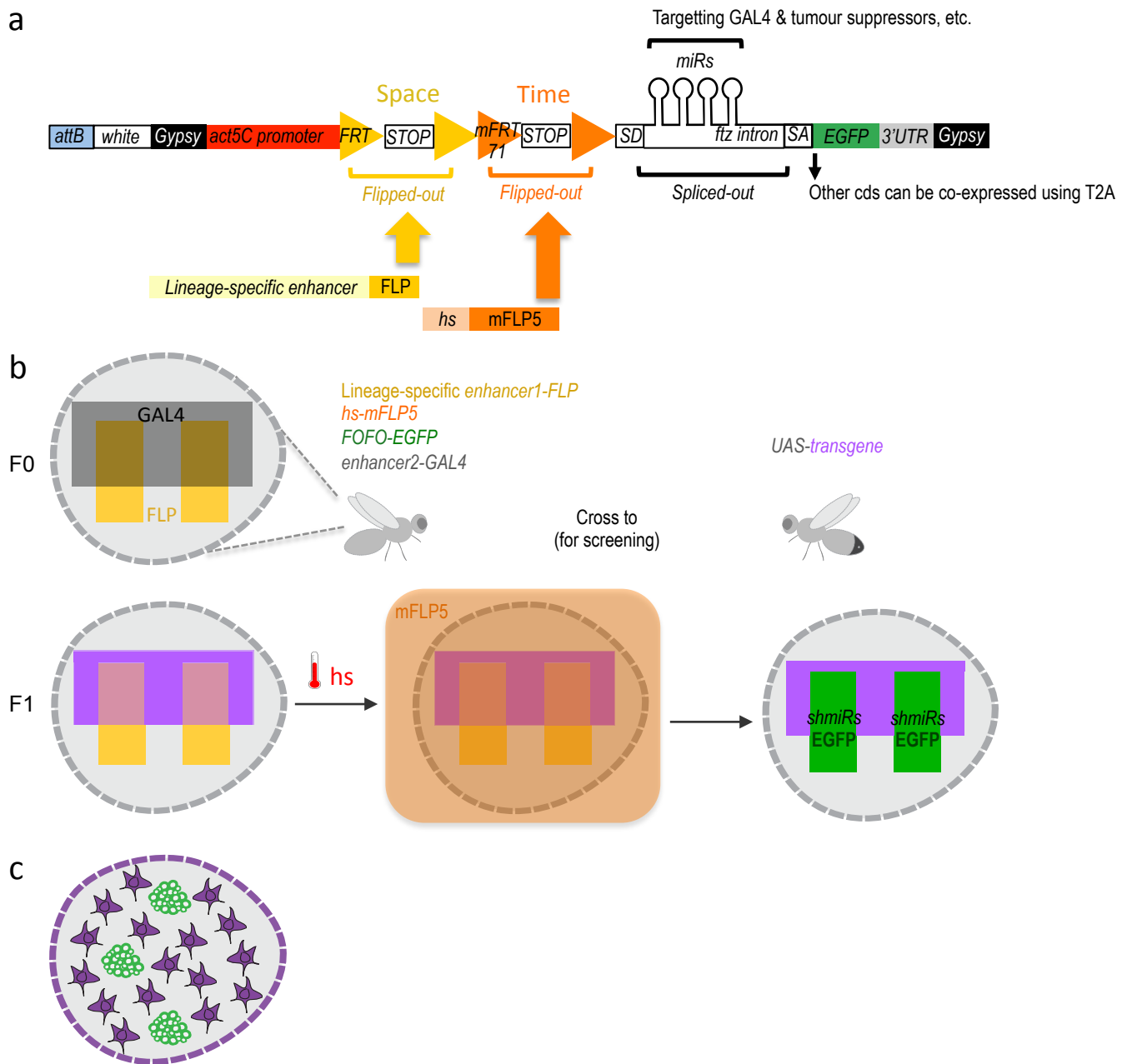


Figure 1 FOFO design and application. **(a)** FOFO construct design: the actin5C promoter is blocked from inducing transcript expression by two efficient transcriptional terminator (STOP) cassettes. Each of these is flanked by FRT or mFRT71, specifically recognized by FLP and mFLP5, respectively. Therefore, miRs and EGFP will only be expressed in cells containing the two flippases. Spatial and temporal control is achieved by providing a spatially restricted FLP and hs-induced mFLP5. SD, splice donor; SA, splice acceptor. Following excision of the *fushi tarazu* (*ftz*) intron, miRs are processed without detriment to reporter expression. Gypsy insulators minimize position effects whilst enhancing expression levels; attB sites allow site-specific insertion into attP-containing host strains. **(b)** Schematic of FOFO application. Expression of deleterious sequences (either knock-down by miRs or overexpression alongside the reporter by means of T2A) can be induced (by heat-shock) in a single fly stock (without need to cross) carrying FOFO, a lineage-specific enhancer1-FLP and hs-mFLP5. The point is then to add in the same flies (F0 generation) a GAL4 transgene (enhancer2-GAL4) and cross to UAS responders. The FOFO containing stock expresses FLP in the spatially restricted domain defined by enhancer1 (yellow) in a tissue represented by the grey shape. FLP expression will constitutively excise the first STOP cassette but the presence of a second STOP cassette precludes expression of anything downstream unless flies are subject to hs. The F1 progeny expresses a transgene (purple) in the GAL4-expressing domain defined by enhancer2 (black). Following hs, mFLP5 expression leads to excision of the second STOP cassette and thus expression of miRs and EGFP in the domain covered by the lineage-specific enhancer. Even if the domain of the latter overlaps with that of enhancer2 as depicted, GAL4 miRs will delete GAL4 expression in the EGFP-expressing domain so that the GAL4 domain never overlaps with that of enhancer1 and only cell non-autonomous effects are assessed. **(c)** Schematic representation of a FOFO application with the tools designed for this study. EGFP-labelled neural tumors (green) are generated within brain lobes (grey shape) in a stock also carrying a GAL4 expressed in glia (purple). Crossing this stock to any UAS-responder lines (could be genome-wide gain- or loss-of function) will allow identification of genes whose glial expression affects tumor size.

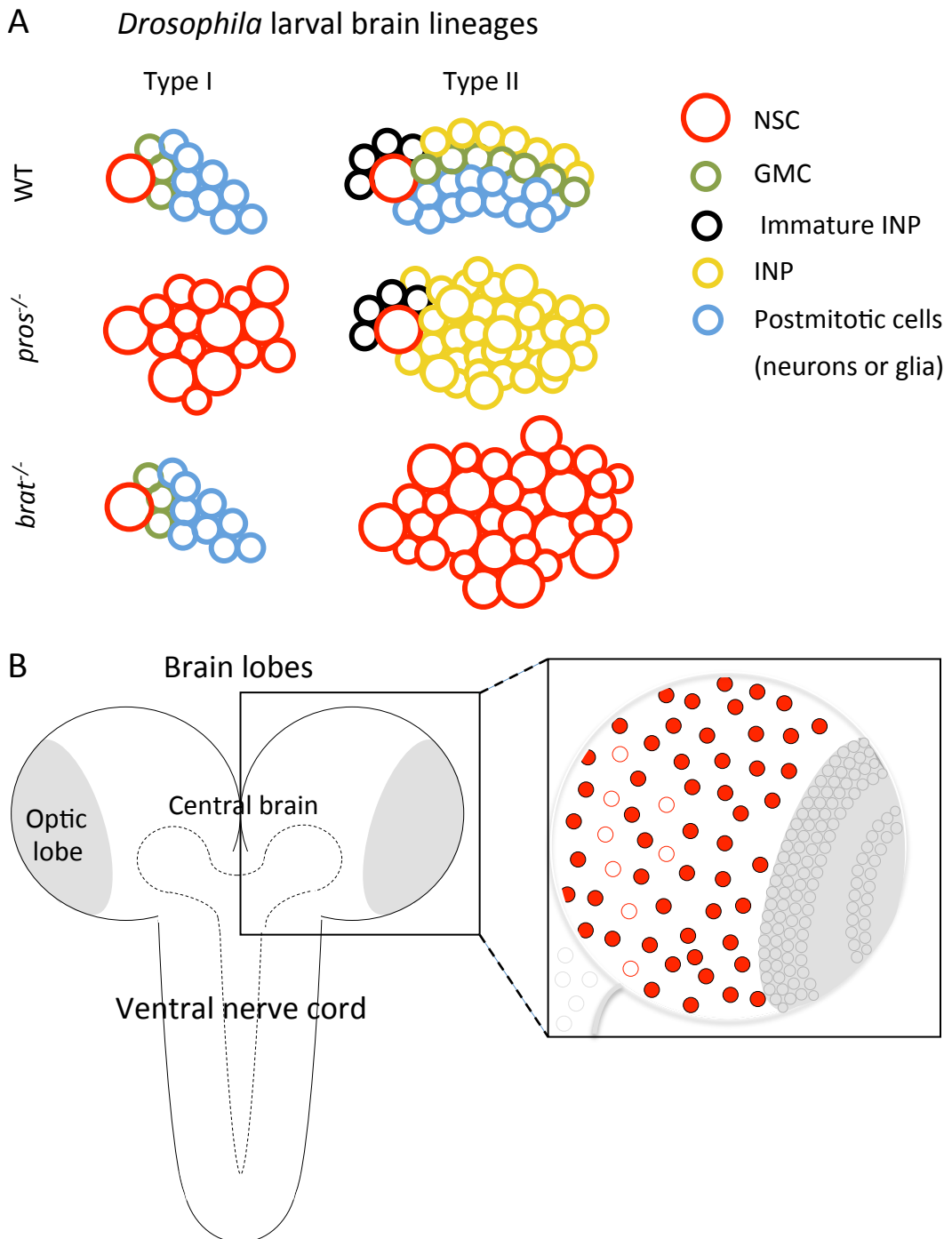


Figure 1–Figure supplement 1. A Schematics of *Drosophila* type I and II larval brain lineages with color-coded cell types; key on the right. NSC, neural stem cells; GMC, ganglion mother cell; INP, intermediate neural progenitor. Wild-type (WT), *pros*^{-/-} and *brat*^{-/-} lineages (tumorigenic) are schematized. In *pros* mutant lineages, GMCs revert to NSCs in type I, and to INPs in type II; *brat* mutation affects only type II lineages, in which INPs revert to NSCs. **B** Schematic of the *Drosophila* CNS and its regionalization: each brain lobe consists of central brain and optic lobe regions; each central brain contains ~100 NSCs: 8 type II (circles outlined in red) and ~90 type I (circles filled in red). Posterior to the brain is the ventral nerve cord (VNC). (Optic lobe and VNC NSCs are represented by grey circles within amplified schematic). The region outlined by dashed line is the neuropil.

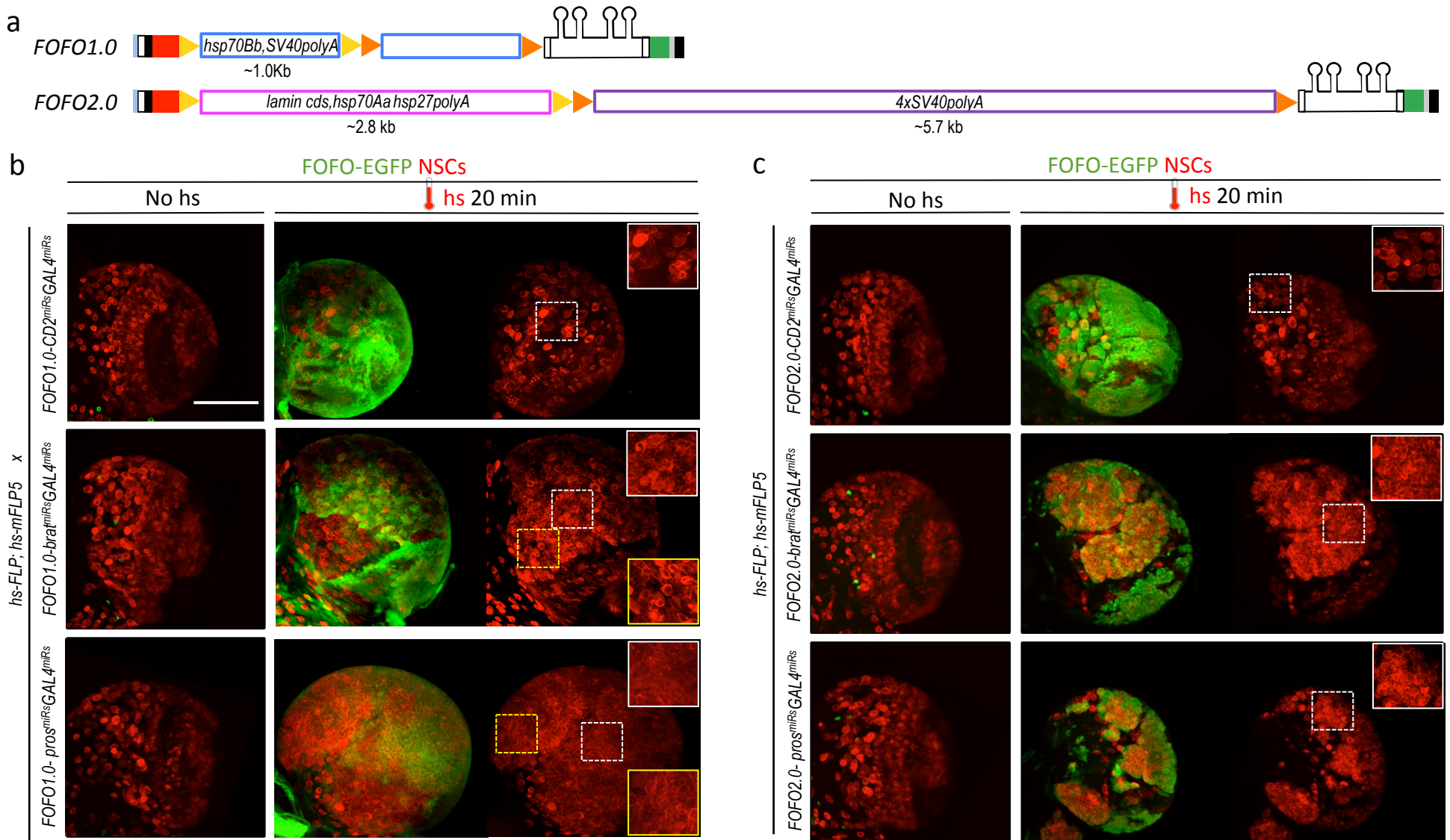


Figure 2 FOFO1.0 versus FOFO2.0. **(a)** FOFO1.0 and FOFO2.0 differ in their STOP cassettes (drawn roughly to scale unlike remainder of construct). **(b)** Wandering third-instar larval brain lobes. In the absence of hs, the brains of animals carrying FOFO1.0 as well as *hs-FLP1* and *hs-mFLP5* look WT. Following hs, miR and EGFP expression is induced and supernumerary NSCs characteristic of these tumors are generated within the EGFP domain (notice NSC density in white-boxed insets). However, supernumerary NSCs outside the EGFP domain were also observed (notice NSC density in yellow-boxed inset, comparable to that of white-boxed inset of same sample). **(c)** Wandering third-instar larval brain lobes. In the absence of hs, the brains of animals carrying FOFO2.0 as well as *hs-FLP1* and *hs-mFLP5* look WT. Following hs, miR and EGFP expression is induced and supernumerary NSCs characteristic of these tumors are generated only within the EGFP domain (white-boxed insets). All images are maximum intensity projections of Z-series but those of brains containing tumors are projections of only a few optical sections. Images are of a representative example obtained from two biological replicates ($n > 10$ per condition). Scale bar: 100 μm .

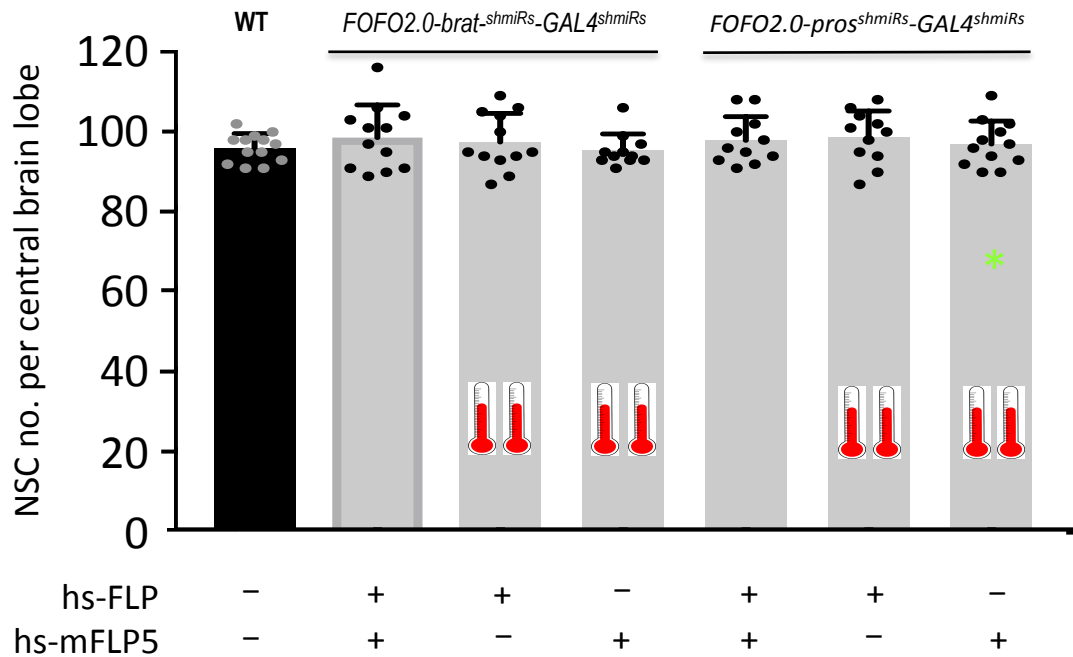


Figure 2–Figure supplement 1 FOF02.0 precludes formation of supernumerary NSCs unless both FLP and mFLP5 are provided. Quantification of the number of NSCs (identified by expression of Miranda) per brain lobe in third-instar larvae of the indicated genotypes (above histograms) crossed to either both hs-FLP and hs-mFLP5 or just one of them (as indicated below graph), subjected or not to heat-shock (indicated by thermometers). One brain lobe per animal was picked at random. Histograms heights represent the mean and error bars the S.D.. There was no statistically significant difference between any of the conditions. Data points shown were collected from two biological replicates (in order of histograms presented: n=13; n=12, p=0.7177; n=12, p=0.964; n=11, p=0.9999; n=11, p=0.9899; n=11, p=0.9995; n=12, p=0.9963).

* At low frequency (0.3 %) tumors were observed in heat-shocked animals carrying only hs-mFLP5 and *FOFO2.0-pros^{shmiRs}-GAL4^{shmiRs}*; tumors were labeled by EGFP expression and in those cases only NSCs outside the green domain were counted.

FOFO-EGFP NSCs All neural lineages

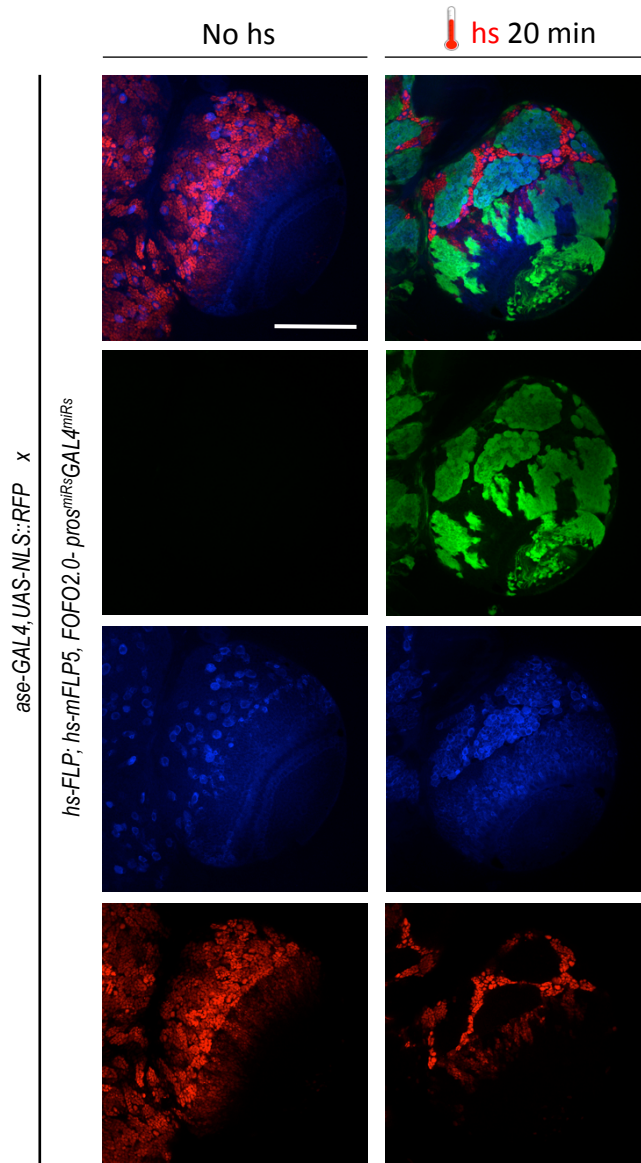


Figure 3 GAL4 miRs efficiently downregulate GAL4. *hs-FLP; hs-mFLP5,FOFO2.0-pros^{miRs}-GAL4^{miRs}* flies were crossed with *ase-GAL4,UAS-NLS::RFP* (which express RFP in all CNS lineages) flies. Wandering third-instar larval brain lobes of progeny are shown. Following heat-shock, EGFP and *GAL4^{miRs}* are expressed by the FOFO construct leading to RFP-negative patches in perfect overlap with EGFP-labeled clones as expected from efficient GAL4 knock-down. Images are of a representative example obtained from two biological replicates (n>10 per condition). Scale bar: 100 μ m.

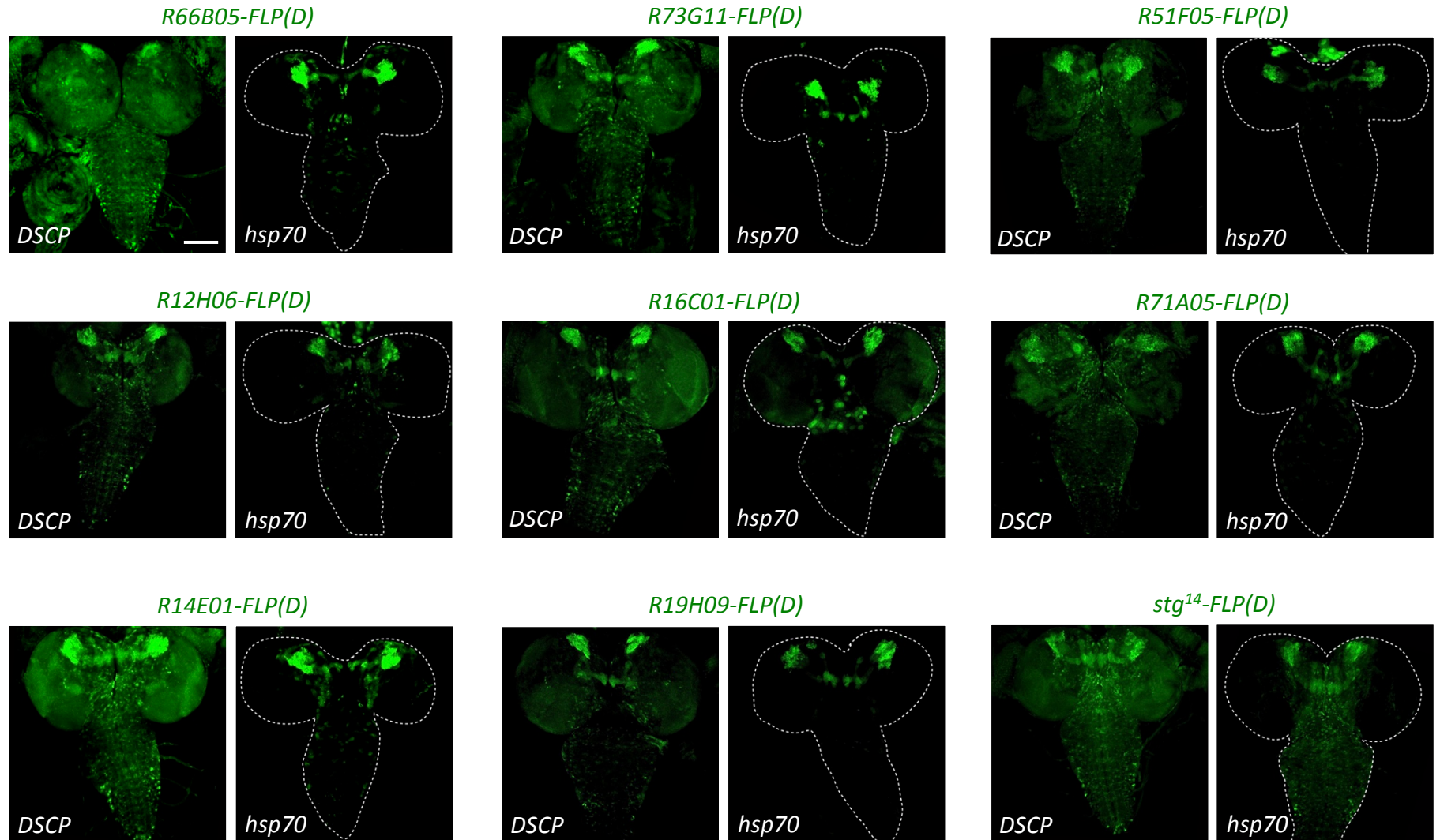


Figure 4 The *hsp70* promoter induces less expression of *enhancer-FLP(D)* lines than the *DSCP* promoter. New *enhancer-FLP(D)* lines were crossed to *act>STOP>GAL4,UAS-GFP* and wandering third-instar larval CNSs imaged for endogenous GFP expression. All genotypes were processed in parallel and imaged with identical conditions. In all cases, expression controlled by the *hsp70* promoter was less relative to that controlled by the *DSCP*, which could be due either to less background or sensitivity. Images are of a representative example obtained from two biological replicates ($n > 10$ per condition). Scale bar: 100 μm .

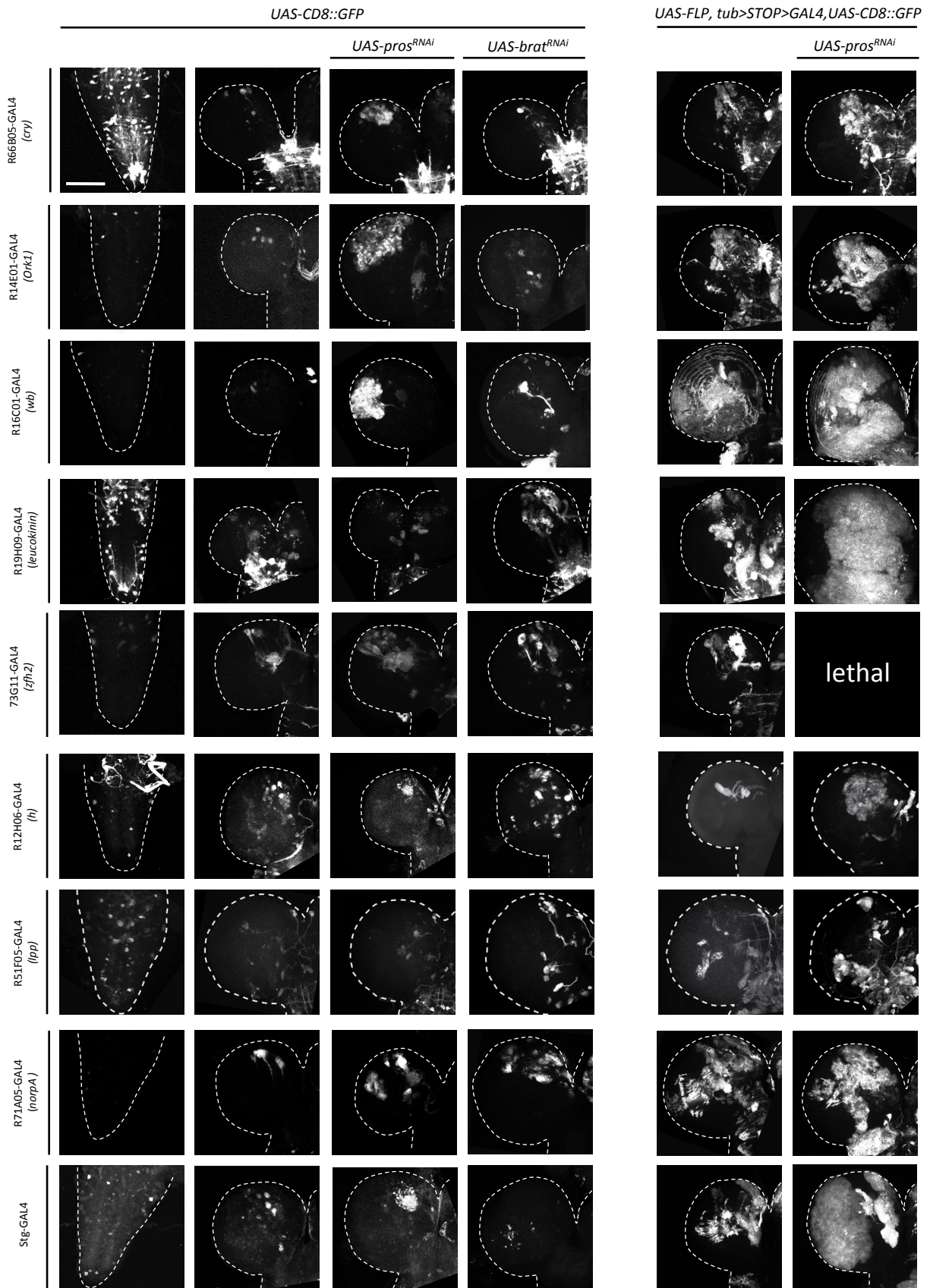


Figure 4—Figure supplement 1. Examples of wandering third-instar larval CNSs of indicated genotypes. The left column contains images of ventral nerve cords and all other images are of brain lobes. All images are maximum intensity projections of Z-series. Images are of a representative example obtained from two biological replicates ($n > 10$ per condition). Scale bar: 100 μm .

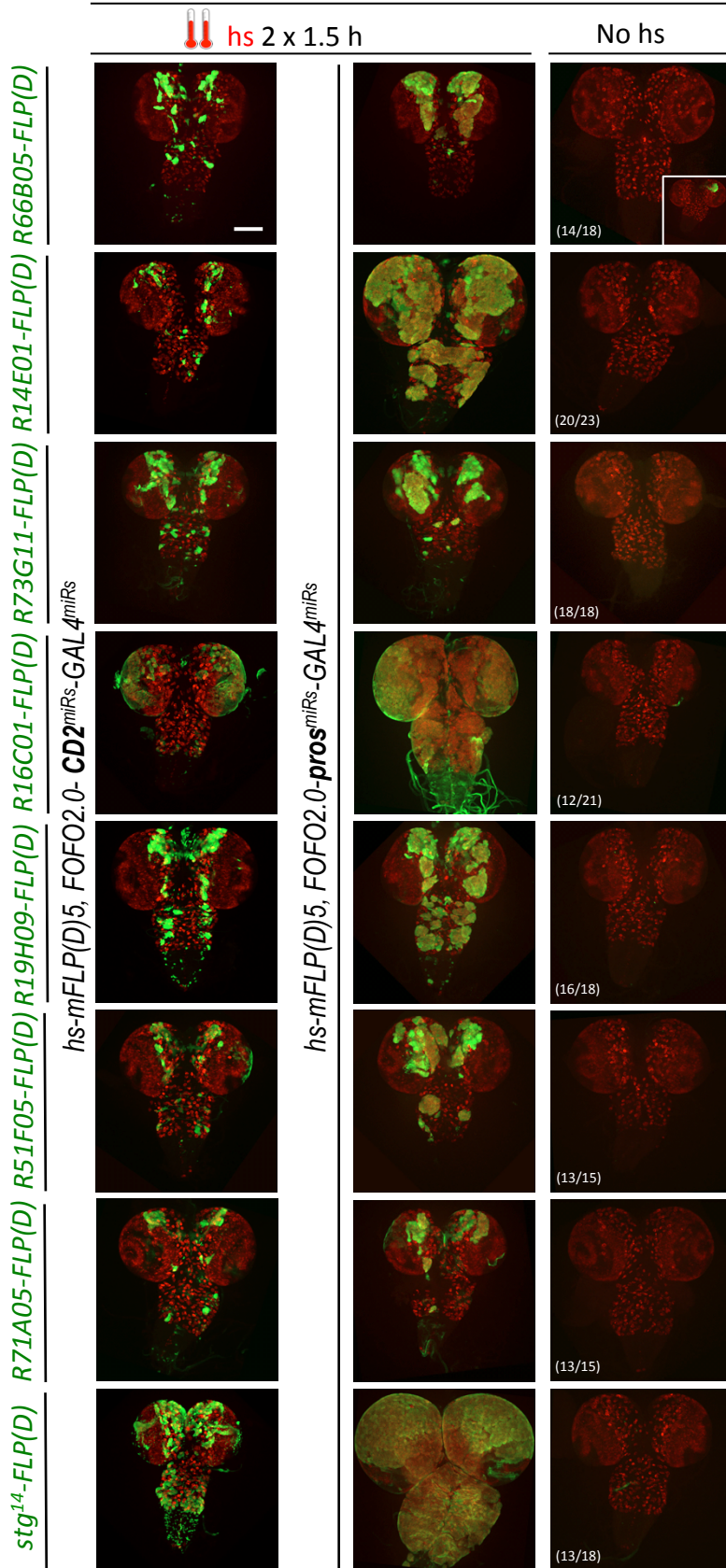


Figure 5 FOF02.0-mediated lineage-restricted CNS tumor generation within a single stock. Shown are wandering third-instar CNSs of hs-induced labeled tumors obtained with eight *enhancer-FLP(D)* and *hs-mFLP5,FOFO2.0-pros^{miRs}-GAL4^{miRs}* compared with non-tumor labeled lineages (same *enhancer-FLP(D)*s with *hs-mFLP5,FOFO2.0-CD2^{miRs}-GAL4^{miRs}*) and background (no hs) tumor incidence. In the absence of heat-shock, tumors were occasionally induced with incomplete penetrance (inset in top right; numbers indicate frequency of CNSs devoid of tumours) but these were much smaller than those intentionally induced by heat-shock. Images are of a representative example obtained from two biological replicates ($n > 10$ per condition and exact number indicated for the background condition – third column). Scale bar: 100 μm .

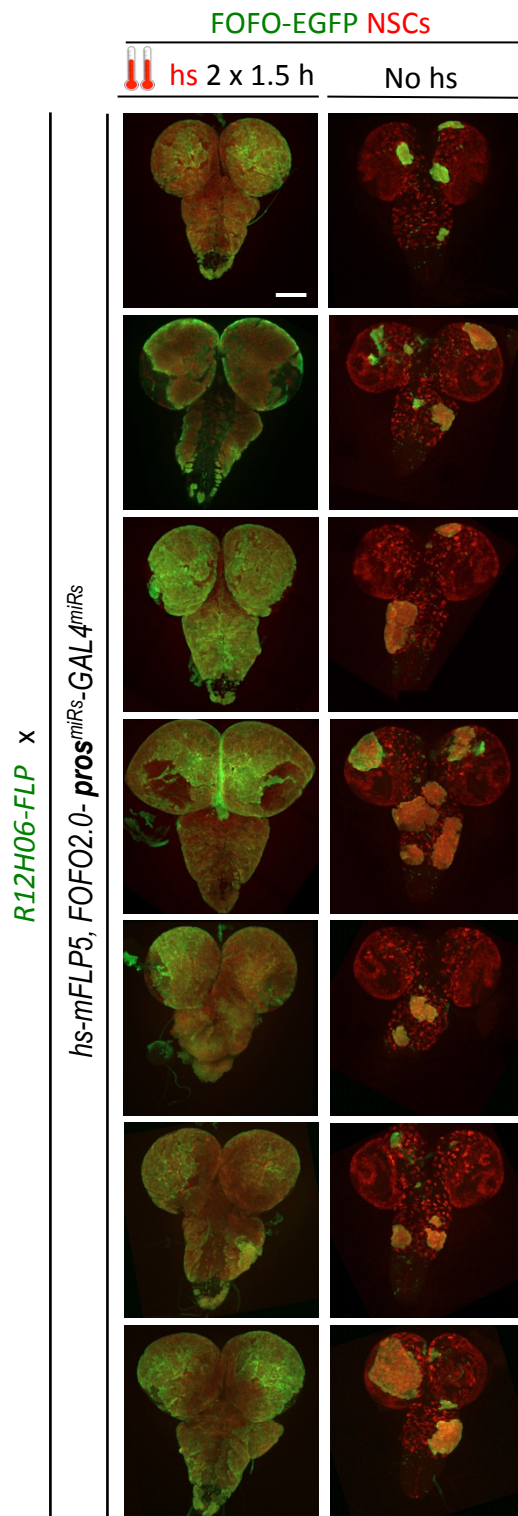


Figure 5–Supplement figure 1 Examples of third-instar larval CNSs from progeny of the cross between indicated genotypes. When subject to heat-shock extensive tumors are induced throughout the CNS (labeled in green and containing supernumerary NSCs). In the absence of heat-shock tumors (albeit much smaller) are induced. All images are maximum intensity projections of Z-series. Images were obtained from two biological replicates (n>13 per condition). Scale bar: 100 μ m.

FOFO-EGFP NSCs

🔥 hs 2 x 1.5 h

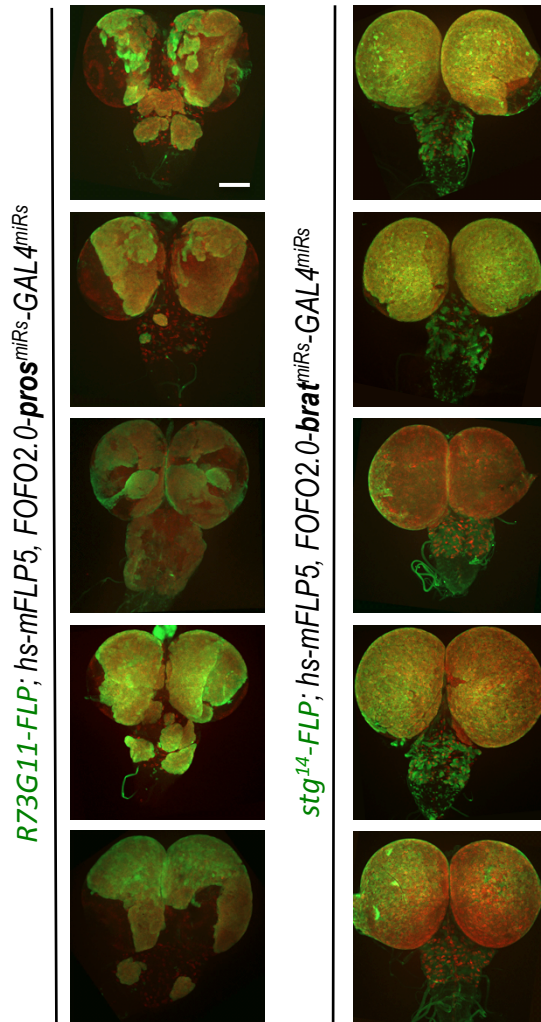



Figure 6 Selection of appropriate enhancer-FLP(D) in combination with hs-mFLP5 allows reproducible CNS tumor generation within a single stock via FOFO2.0. Shown are white prepupal CNSs (compare with analogous enhancers in Fig. 5 driving FOFO2.0 containing CD2^{miRs}). Images were obtained from two biological replicates (n=6 for left column; n=16 for right). Scale bar: 100 μ m.

FOFO-EGFP NSCs

 hs 2 x 1.5 h

R19H09-FLP; hs-mFLP5, FOFO2.0-brat^{shmiRs}-GAL4^{shmiRs}

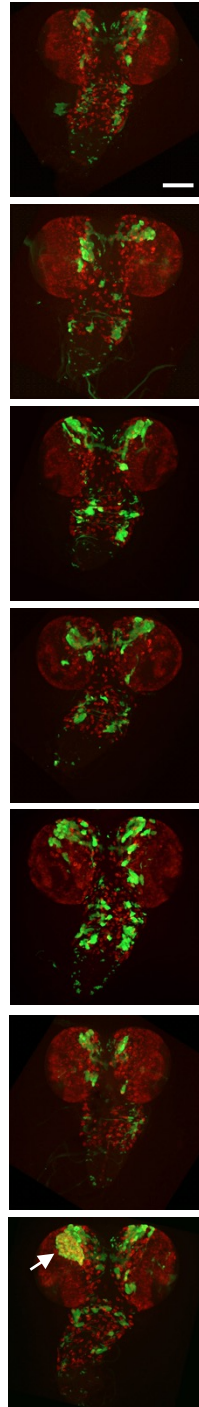


Figure 6–Supplement Figure 1 Examples of third-instar larval CNSs from a stable stock of the indicted genotype subject to heat-shock. Small tumors are only occasionally induced in this genotype (arrow). All images are maximum intensity projections of Z-series. Images were obtained from two biological replicates (n=14). Scale bar: 100 μ m.